AIAA JOURNAL
Vol. 39, No. 4, April 2001

Design Potential Method for Robust System Parameter Design

Jian Tu*
General Motors Research and Development Center, Warren, Michigan 48090
Kyung K. Choi†
University of Iowa, Iowa City, Iowa 52242
and
Young H. Park‡
New Mexico State University, Las Cruces, New Mexico 88003

A novel design potential method that integrates the probabilistic constraint evaluation closely into the design optimization process is presented for robust system parameter design. From a broader perspective, it is shown that the probabilistic constraints can be evaluated using either the conventional reliability index approach or the proposed performance measure approach. The performance measure approach is inherently robust and is more effective when the probabilistic constraint is inactive. The reliability index approach is more effective for the violated probabilistic constraint, but it could yield singularity when the probabilistic constraint is inactive. Moreover, the close coupling of performance probability analysis and design optimization is illustrated in a proposed unified system space. The design potential method, which is developed to take full advantage of the important design information obtained from the previous probabilistic constraint evaluation, can significantly accelerate the convergence of the reliability-based design optimization process.

Nomenclature

$\boldsymbol{d}$ = system design variables, $d_1, d_2, \ldots, d_n]^T$
$\boldsymbol{d}_P^k$ = design potential point (DPP) for design potential method at design $\boldsymbol{d}^k$
$F_G(\,)$ = cumulative distribution function (CDF) of the system performance function $G(\boldsymbol{x})$, $F_G(g)$ is equal to $P\ G(\boldsymbol{x}) < g]$
$F_G^{-1}(\,)$ = inverse of the CDF of $G(\boldsymbol{x})$
$F_{X_i}(x_i)$ = CDF of a random system parameter X_i
$f_X(\boldsymbol{x})$ = joint PDF of the random system parameters
$f_{X_i}(x_i)$ = probability density function (PDF) of a random system parameter X_i
$G(\boldsymbol{x})$ = system performance function; system is considered failed if $G(\boldsymbol{x}) < 0$
g = probabilistic performance measure of $G(\boldsymbol{x})$
g^* = target probabilistic performance measure, equal to $F_G^{-1}(\bar{P}_f)$ and $F_G^{-1}\ \Phi(-\beta_t)]$
$P(\,)$ = probability function
P_f = failure probability of a system performance function, equal to $P\ G(\boldsymbol{x}) < 0]$
$\bar{P}_f$ = prescribed failure probability limit for a system performance function
$\boldsymbol{T}(\boldsymbol{x}; \boldsymbol{d}^k)$ = transformation in first-order reliability method (FORM) at design $\boldsymbol{d}^k$
$\boldsymbol{T}^{-1}(\boldsymbol{u}; \boldsymbol{d}^k)$ = inverse transformation in FORM at design $\boldsymbol{d}^k$
$\boldsymbol{u}$ = independent, standardized normal random variables, $u_1, u_2, \ldots, u_n]^T$
$\boldsymbol{u}^*_{g=0}$ = most probable point (MPP) in the first-order reliability analysis of reliability index approach (RIA)
$\boldsymbol{u}^*_{\beta=\beta_t}$ = MPP in the first-order inverse reliability analysis of performance measure approach (PMA)
$\boldsymbol{X}$ = random system parameters, $X_1, X_2, \ldots, X_n]^T$
$\boldsymbol{x}$ = outcomes of $\boldsymbol{X}$, $x_1, x_2, \ldots, x_n]^T$
$\boldsymbol{x}^*_{g=0}$ = MPP of RIA in $\boldsymbol{x}$ space; $G(\boldsymbol{x}^*_{g=0}) = 0$ and $\|\boldsymbol{u}^*_{g=0}\| = \|\boldsymbol{T}(\boldsymbol{x}^*_{g=0}; \boldsymbol{d}^k)\| = \beta_s$
$\boldsymbol{x}^*_{\beta=\beta_t}$ = MPP of PMA in $\boldsymbol{x}$ space; $G(\boldsymbol{x}^*_{\beta=\beta_t}) = g^*$ and $\|\boldsymbol{u}^*_{\beta=\beta_t}\| = \|\boldsymbol{T}(\boldsymbol{x}^*_{\beta=\beta_t}; \boldsymbol{d}^k)\| = \beta_t$
β_s = reliability index, equal to $-\Phi^{-1}(P_f) = -\Phi^{-1}\ F_G(0)]$
β_t = target reliability index for a system performance function, equal to $-\Phi^{-1}(\bar{P}_f)$
$\boldsymbol{\mu}$ = mean values of random system parameters $\boldsymbol{X}$, $\mu_1, \mu_2, \ldots, \mu_n]^T$
$\Phi^{-1}(\,)$ = inverse of the standard normal CDF $\Phi(\,)$

Introduction

THE existence of uncertainties in either engineering simulations or manufacturing processes requires a reliability-based design optimization (RBDO) model for robust and cost-effective designs. In the RBDO model, the mean values and the standard deviations of random system parameters can be chosen as design variables, and the cost function is minimized subject to prescribed probabilistic constraints. In practical applications, however, the RBDO processes are often simplified and divided into two phases[1,2] as the system parameter design and the parameter tolerance design. In robust system parameter design, the mean values are optimized subject to given tolerances of the random system parameters by solving a mathematical nonlinear programming problem. The parameter tolerance design can then be performed through tradeoff and what-if studies to reallocate the standard deviations of random system parameters so that the cost can be further reduced.

In the conventional RBDO methodology for system parameter design, the probabilistic constraints are directly prescribed by the reliability indexes evaluated in the traditional first-order reliability analysis.[3–9] The RBDO problem is often solved by the search method[10,11] for constrained nonlinear optimization, where the search direction is evaluated by solving an optimization subproblem defined by the linearized probabilistic constraints at the current design.

However, the reliability index approach (RIA) represents only one perspective of the probabilistic constraints. From a broader perspective, it is shown that the probabilistic constraint can also be evaluated using the proposed[12] performance measure approach (PMA), where the value of the performance function at the target most probable point (design point) is obtained using an inverse reliability

Received 13 September 1999; revision received 5 September 2000; accepted for publication 8 September 2000.

*Senior Research Engineer, Vehicle Analysis and Dynamics Laboratory, 30500 Mound Road; jian.tu@gm.com.
†Professor and Director, Center for Computer-Aided Design and Department of Mechanical Engineering, College of Engineering; kkchoi@ccad.uiowa.edu.
‡Assistant Professor, Department of Mechanical Engineering; ypark@nmsu.edu.

analysis. The PMA is inherently robust and is more efficient if the probabilistic constraint is inactive. In contrast, RIA may be more effective when the probabilistic constraint is violated, but it could yield singularity for the inactive probabilistic constraint. Thus, an adaptive probabilistic constraint evaluation strategy[13] is proposed for robustness and efficiency, where one of the two approaches is selected, depending on the estimated marginal status of the probabilistic constraint.

More important, probability analysis in the probabilistic constraint evaluation is closely coupled with the overall RBDO process, and their connection can be illustrated in the proposed unified system space. By integrating probabilistic constraint evaluation closely into the design optimization process, a novel design potential method (DPM) is proposed for effective RBDO applications. For DPM, a design potential point (DPP) is defined as the design that renders the probabilistic constraint active. The probabilistic constraint is then linearized at its DPP in defining the search direction determination subproblem. Because DPP is on the limit-state surface of the probabilistic constraint, DPM provides better constraint approximation than the traditional linerization at the current design and, therefore, significantly improves the convergence rate of RBDO.

Random System Parameter and System Performance Function

An engineering system can be described by a set of continuous random system parameters, $\boldsymbol{X} = [X_i]^T$, $i = 1, 2, \ldots, n$. The statistical description of a system parameter X_i can be characterized by its cumulative distribution function (CDF) $F_{X_i}(x_i)$ or probability density function (PDF) $f_{X_i}(x_i)$ as[14]

$$F_{X_i}(x_i) = P(X_i < x_i) = \int_{x_i^L}^{x_i} f_{X_i}(x_i)\,\mathrm{d}x, \qquad x_i^L \le x_i \le x_i^U \tag{1}$$

where x_i^L and x_i^U are called the tolerance limits of X_i and are often finite. The probability distribution of X_i can be partially described by some characteristic factors, such as its mean value μ_i and variance σ_i^2. In robust system parameter design, the mean values of some random system parameters are often used as independent design variables, whereas their other characteristic factors are either constants or depend on the mean values, for example,

$$\boldsymbol{d} = [d_i]^T \equiv [\mu_i]^T, \qquad i = 1, 2, \ldots, n \tag{2}$$

$$\sigma_i^2 = \sigma_i^2(\mu_i) = \sigma_i^2(d_i), \qquad i = 1, 2, \ldots, n \tag{3}$$

The system performance criteria are described by system performance functions. Consider a system performance function $G(\boldsymbol{x})$, where the system fails if $G(\boldsymbol{x}) < 0$. The statistic description of $G(\boldsymbol{x})$ is then characterized by its CDF $F_G(g)$ as

$$F_G(g) = P[G(\boldsymbol{x}) < g] = \int_{G(\boldsymbol{x})<g} \cdots \int f_X(\boldsymbol{x})\,\mathrm{d}x_1, \ldots, \mathrm{d}x_n$$

$$\boldsymbol{x}^L \le \boldsymbol{x} \le \boldsymbol{x}^U \tag{4}$$

where g is the probabilistic performance measure and $f_X(\boldsymbol{x})$ is the joint PDF (JPDF) of the system parameters. The probability integration domain is bounded by the tolerance limits of the random system parameters $\boldsymbol{x}^L$ and $\boldsymbol{x}^U$. Note that $F_G(g)$ is a nondecreasing function of g, and the failure probability corresponding to this system performance is

$$P_f = P[G(\boldsymbol{x}) < 0] = F_G(0) \tag{5}$$

RBDO Model

In practical applications that the safety constraints can be imposed on the reliabilities of the individual failure modes, the RBDO model for robust system parameter design is generally defined as follows[3–9]:
Minimize

$$\mathrm{cost}(\boldsymbol{d}) \tag{6a}$$

subject to

$$P_{f,j} = P[G_j(\boldsymbol{x}) < 0] \le \bar{P}_{f,j}, \qquad j = 1, 2, \ldots, np \tag{6b}$$

$$\boldsymbol{d}^L \le \boldsymbol{d} \le \boldsymbol{d}^U \tag{6c}$$

where $\bar{P}_{f,j}$ is the prescribed failure probability limit for the jth system performance function and np is the total number of probabilistic constraints.

The failure probability limit can be represented by the reliability target index, $\beta_t = -\Phi^{-1}(\bar{P}_f)$. Hence, the probabilistic constraint in Eq. (6b) can be rewritten using Eq. (5) as

$$F_G(0) \le \Phi(-\beta_t) \tag{7a}$$

which can be expressed in two ways through inverse transformations as[15,16]

$$\beta_s = -\Phi^{-1}[F_G(0)] \ge \beta_t \tag{7b}$$

$$g^* = F_G^{-1}[\Phi(-\beta_t)] \ge 0 \tag{7c}$$

where β_s is traditionally called the reliability index and g^* is the target probabilistic performance measure[12] as illustrated by the next example in Fig. 1.

To date, most researchers used the RIA[3–9] in Eq. (7b) to prescribe directly the probabilistic constraint as

$$\beta_s(\boldsymbol{d}) \ge \beta_t \tag{8a}$$

It was clearly shown earlier that Eq. (7c) can also be used to prescribe the probabilistic constraint, and it is called the PMA with the constraint[12]

$$g^*(\boldsymbol{d}) \ge 0 \tag{8b}$$

At a given design $\boldsymbol{d}^k = [d_i^k]^T = [\mu_i^k]^T$, the evaluation of $\beta_s(\boldsymbol{d}^k)$ in RIA is called the reliability analysis and the evaluation of $g^*(\boldsymbol{d}^k)$ in PMA is called the inverse reliability analysis, that is,

$$\beta_s(\boldsymbol{d}^k) = -\Phi^{-1}\left[\int_{G(\boldsymbol{x})<0} \cdots \int f_X(\boldsymbol{x})\,\mathrm{d}x_1, \ldots, \mathrm{d}x_n\right]$$

$$x_i^L \le x_i \le x_i^U \tag{9a}$$

$$g^*(\boldsymbol{d}^k) = F_G^{-1}\left[\int_{G(\boldsymbol{x})<g^*} \cdots \int f_X(\boldsymbol{x})\,\mathrm{d}x_1, \ldots, \mathrm{d}x_n\right]$$

$$x_i^L \le x_i \le x_i^U \tag{9b}$$

Example 1

Consider a system described by two independent, uniformly distributed random system parameters, $X_i \sim \mathrm{uniform}[a_i, b_i]$, $i = 1, 2$, and their PDFs as

$$f_{X_i}(x_i) = 1/(b_i - a_i), \qquad a_i \le x_i \le b_i, \qquad i = 1, 2 \tag{10a}$$

where the mean values and variances of system parameters are expressed, respectively, as

$$\mu_i = \int_{a_i}^{b_i} x_i f_{X_i}(x_i)\,\mathrm{d}x_i = \frac{b_i - a_i}{2}, \qquad i = 1, 2 \tag{10b}$$

$$\sigma_i^2 = \int_{a_i}^{b_i} (x_i - \mu_i)^2 f_{X_i}(x_i)\,\mathrm{d}x_i = \frac{(b_i - a_i)^2}{12}, \qquad i = 1, 2 \tag{10c}$$

Both μ_1 and μ_2 are chosen as design variables, $\boldsymbol{d} = [d_1, d_2]^T \equiv [\mu_1, \mu_2]^T$, and variances are constants as $\sigma_1^2 = \sigma_2^2 = \frac{1}{3}$. Thus, the PDFs of system parameters can be expressed in terms of design variables as

$$f_{X_i}(x_i) = \tfrac{1}{2}, \qquad d_i - 1 \le x_i \le d_i + 1, \qquad i = 1, 2 \tag{10d}$$

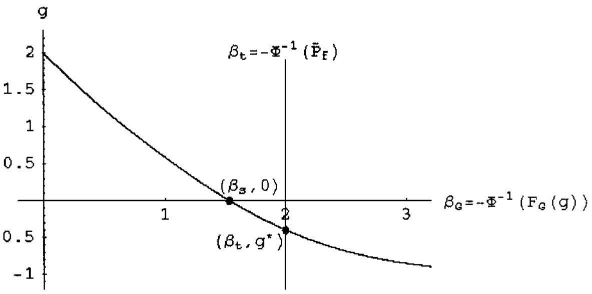

Fig. 1 Probabilistic constraint evaluation by RIA and PMA.

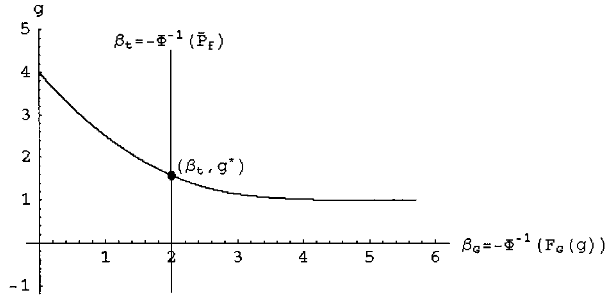

Fig. 2 Difference of RIA and PMA in constraint evaluation.

Because X_1 and X_2 are independent, their JPDF can be explicitly expressed as

$$f_X(\boldsymbol{x}) = f_{X_1}(x_1) f_{X_2}(x_2) = \tfrac{1}{4}$$
$$d_i - 1 \le x_i \le d_i + 1, \qquad i = 1, 2 \tag{10e}$$

Consider a probabilistic constraint of the RBDO model that is defined as

$$P\; G(\boldsymbol{X}) < 0] \le 0.02275 = \Phi(-\beta_t) \tag{10f}$$

where $\beta_t = -\Phi^{-1}(0.02275) = 2$. The system performance function and its CDF are

$$G(\boldsymbol{x}) = x_1 + 2x_2 - 10 \tag{10g}$$

$$F_G(g) = \frac{1}{4}\int_{G(x)<g} \cdots \int \mathrm{d}x_1, \ldots, \mathrm{d}x_n$$
$$d_i - 1 \le x_i \le d_i + 1, \qquad i = 1, 2 \tag{10h}$$

Case 1: Consistency of RIA and PMA in Probabilistic Constraint Evaluation

The CDF $F_G(g)$ for a given design can be exemplified by performing the multiple probability integration of Eq. (10h) repeatedly with different g values. When $F_G(g)$ is transformed to the general probability index, $\beta_G(g) = -\Phi^{-1}\; F_G(g)]$, the nonincreasing $\beta_G \sim g$ curve of the design $\boldsymbol{d}^k = \; 4, 4]^T$ is shown in Fig. 1.

The probabilistic constraint evaluation is to exemplify a point on the nonincreasing $\beta_G \sim g$ curve that can sufficiently identify the current status of the probabilistic constraint. In the conventional RIA, the point (β_s, 0) is exemplified by the reliability analysis of Eq. (9a). From another perspective, the point (β_t, g^*) is exemplified by the inverse reliability analysis of Eq. (9b) in the proposed PMA.

In this example, the probabilistic constraint is violated at design $\boldsymbol{d}^k$, which can be identified by both RIA and PMA, respectively, as

$$\beta_s(\boldsymbol{d}^k) = \beta_G(0) = -\Phi^{-1}\; F_G(0)] = 1.512 < \beta_t = 2 \tag{10i}$$

$$g^*(\boldsymbol{d}^k) = g(\beta_t) = F_G^{-1}\; \Phi(-\beta_t)] = -0.452 < 0 \tag{10j}$$

Case 2: Difference of RIA and PMA in Probabilistic Constraint Evaluation

As shown in Fig. 1, RIA and PMA exemplify two distinct points that become coincident if and only if the probabilistic constraint is active, that is, $\beta_s = \beta_t$ and $g^* = 0$. Hence, the computational costs of RIA and PMA are generally different. Moreover, it will be explained in the rest of this section that PMA is inherently robust, whereas RIA could yield singularity in the probabilistic constraint evaluation.

The nonincreasing $\beta_G \sim g$ curve of another design $\boldsymbol{d}^m = \; 4, 5]^T$ is shown in Fig. 2. Note that point (β_s, 0) does not exist on the $\beta_G \sim g$ curve because the failure probability of this design is zero. Numerically, the reliability index $\beta_s(\boldsymbol{d}^k)$ approaches infinity, and thus RIA yields singularity. In contrast, the target probabilistic performance measure g^* of PMA can always be obtained. Although RIA also yields singularity if the failure probability of the design $\boldsymbol{d}^m$ is 100%, that is, $\beta_s(\boldsymbol{d}^m)$ approaches negative infinity, any highly unreliable design $\boldsymbol{d}^m$ with negative $\beta_s(\boldsymbol{d}^m)$ can be easily avoided[13] in the RBDO process.

Approximate Probability Integration in Constraint Evaluation

The probabilistic constraint can be evaluated from different perspectives,[12] where RIA and PMA are two special cases. The exact reliability analysis of Eq. (9a) in RIA and the exact inverse reliability analysis of Eq. (9b) in PMA involve multiple probability integration that is in general extremely complicated to compute.

In practice, the first-order reliability method (FORM) can be used to provide efficient and adequate approximation solutions for engineering probability analysis.[15] In FORM, the general one-to-one transformations between the dependent, nonnormal system parameters $\boldsymbol{X}$ ($\boldsymbol{x}$ space) and the independent, standardized normal variables $\boldsymbol{U}$ ($\boldsymbol{u}$ space) at a given design $\boldsymbol{d}^k$ can be expressed as[15,17,18]

$$\boldsymbol{u} = \; u_i]^T = \boldsymbol{T}(\boldsymbol{x}; \boldsymbol{d}^k) = \left[T_i(\boldsymbol{x}; \boldsymbol{d}^k)\right]^T \tag{11a}$$

$$\boldsymbol{x} = \; x_i]^T = \boldsymbol{T}^{-1}(\boldsymbol{u}; \boldsymbol{d}^k) = \left[T_i^{-1}(\boldsymbol{u}; \boldsymbol{d}^k)\right]^T \tag{11b}$$

If all system parameters are mutually independent, the one-to-one transformation can be expressed separately for each system parameter as

$$u_i = T_i\left(x_i; d_i^k\right) = \Phi^{-1}\left[F_{X_i}(x_i)\right], \qquad i = 1, 2, \ldots, n \tag{11c}$$

$$x_i = T_i^{-1}\left(u_i; d_i^k\right) = F_{X_i}^{-1}\; \Phi(u_i)], \qquad i = 1, 2, \ldots, n \tag{11d}$$

The performance function $G(\boldsymbol{x})$ can then be expressed in the $\boldsymbol{u}$ space as

$$G(\boldsymbol{x}) = G\; \boldsymbol{T}^{-1}(\boldsymbol{u}; \boldsymbol{d}^k)] = G_U(\boldsymbol{u}) \tag{12}$$

General Interpretation of FORM[15]

In the $\boldsymbol{u}$ space, the point on the surface $G_U(\boldsymbol{u}) = \bar{g}$ with the maximum joint probability density is the point with the minimum distance from the origin. The point $\boldsymbol{u}^*_{g=\bar{g}}$ is called the most probable point (MPP), and the minimum distance $\|\boldsymbol{u}^*_{g=\bar{g}}\|$ is defined in FORM as the first-order probability index $\beta_{\mathrm{FORM}}(\bar{g})$, which represents the first-order approximation of the general probability index $\beta_G(\bar{g})$ as

$$\beta_{\mathrm{FORM}}(\bar{g}) \approx \beta_G(\bar{g}) = -\Phi^{-1}\; F_G(\bar{g})]$$
$$= -\Phi^{-1}\left[\int_{G(x)<\bar{g}} \cdots \int f_X(\boldsymbol{x})\, \mathrm{d}x_1, \ldots, \mathrm{d}x_n\right]$$
$$x_i^L \le x_i \le x_i^U \tag{13}$$

First-Order Reliability Analysis in RIA

The first-order reliability index $\beta_{s,\mathrm{FORM}}(\boldsymbol{d}^k)$ is defined in the $\boldsymbol{u}$ space as the distance from the MPP $\boldsymbol{u}^*_{g=0}$ on the performance function limit-state surface, $G_U(\boldsymbol{u}) = 0$, to the origin, that is, $\beta_{s,\mathrm{FORM}}(\boldsymbol{d}^k) = \|\boldsymbol{u}^*_{g=0}\|$. Thus, the first-order reliability analysis can be performed by solving a nonlinear optimization problem in the $\boldsymbol{u}$ space as follows[15]:

Minimize

$$\|\boldsymbol{u}\| \tag{14a}$$

subject to

$$G_U(\boldsymbol{u}) = 0 \tag{14b}$$

which can also be represented directly in the $\boldsymbol{x}$ space using Eq. (11a) and Eq. (12) as follows:
Minimize

$$\|\boldsymbol{T}(\boldsymbol{x}; \boldsymbol{d}^k)\| \tag{14c}$$

subject to

$$G(\boldsymbol{x}) = 0 \tag{14d}$$

$$\boldsymbol{x}^L \leq \boldsymbol{x} \leq \boldsymbol{x}^U \tag{14e}$$

where the optimum solution $\boldsymbol{x}^*_{g=0} = \boldsymbol{T}^{-1}\ (\boldsymbol{u}^*_{g=0}; \boldsymbol{d}^k)$ is called MPP of RIA in the $\boldsymbol{x}$ space.

Note that the first-order reliability analysis is defined in the probability integration domain of Eq. (14e), which is usually bounded by the finite tolerance limits of system parameters. Because the failure probability is zero if $G(\boldsymbol{x})$ is positive everywhere in this integration domain, Eq. (14e) can also be represented as $\|\boldsymbol{T}(\boldsymbol{x}; \boldsymbol{d}^k)\| \leq -\Phi^{-1}(0) \to \infty$.

First-Order Inverse Reliability Analysis in PMA

The first-order target probabilistic performance measure is defined in the $\boldsymbol{u}$ space as the performance function value at the MPP $\boldsymbol{u}^*_{\beta=\beta_t}$ that renders the distance β_t from the origin, that is, g^*_{FORM} $(\boldsymbol{d}^k) = G_U(\boldsymbol{u}^*_{\beta=\beta_t})$. The first-order inverse reliability analysis can also be performed by solving a nonlinear optimization problem[12] in the $\boldsymbol{u}$ space as follows:
Minimize

$$G_U(\boldsymbol{u}) \tag{15a}$$

subject to

$$\|\boldsymbol{u}\| = \beta_t \tag{15b}$$

which is illustrated by the next example in Fig. 3 and can also be represented directly in the x space using Eq. (11b) and Eq. (12) as follows:
Minimize

$$G(\boldsymbol{x}) \tag{15c}$$

subject to

$$\|\boldsymbol{T}(\boldsymbol{x}; \boldsymbol{d}^k)\| = \beta_t \tag{15d}$$

where the optimum solution $\boldsymbol{x}^*_{\beta=\beta_t} = \boldsymbol{T}^{-1}(\boldsymbol{u}^*_{\beta=\beta_t}; \boldsymbol{d}^k)$ is called MPP of PMA in the $\boldsymbol{x}$ space. Because of the finite value of β_t in Eq. (15d), the inverse reliability analysis is always performed in the probability integration domain defined by Eq. (14e).

Numerical Algorithms for MPP Search in RIA and PMA

General constrained optimization algorithms,[19] such as sequential linear programming (SLP), sequential quadratic programming (SQP), method of feasible directions (MFD), gradient projection method, and augmented Lagrangian method, can be used for the MPP search in either RIA or PMA. Many specialized MPP search algorithms,[20–24] such as HL-RF (Hasofer–Lind–Rackwitz–Fiessler Method), modified HL-RF, and AMVFO (Advanced Mean Value First Order Method), have been developed for RIA. AMVFO+ can also be used for efficient MPP search in PMA.

Example 2

Consider the same system as in example 1, where the system parameter CDFs are

$$F_{X_i}(x_i) = (x_i - a_i)/(b_i - a_i) = (x_i - d_i + 1)/2$$
$$d_i - 1 \leq x_i \leq d_i + 1, \qquad i = 1, 2 \tag{16a}$$

In FORM, the transformations between the $\boldsymbol{x}$ space and the $\boldsymbol{u}$ space at design $\boldsymbol{d}^k$ of the two independent uniformly distributed system parameters are

$$u_i = T_i\left(x_i; d_i^k\right) = \Phi^{-1}\left[F_{X_i}(x_i)\right] = \Phi^{-1}\ (x_i - d_i + 1)/2] \qquad i = 1, 2 \tag{16b}$$

$$x_i = T_i^{-1}\left(u_i; d_i^k\right) = F_{X_i}^{-1}\ \Phi(u_i)] = d_i^k - 1 + 2\Phi(u_i) \qquad i = 1, 2 \tag{16c}$$

and the performance function is expressed in the $\boldsymbol{u}$ space as

$$G_U(\boldsymbol{u}) = 2\Phi(u_1) + 4\Phi(u_2) + d_1^k + 2d_2^k - 13 \tag{16d}$$

For illustration, the MPP locus[20,21] in the $\boldsymbol{u}$ space can be obtained if the first-order inverse reliability analysis is performed repeatedly for different β values as follows:
Minimize

$$G_U(\boldsymbol{u}) \tag{16e}$$

subject to

$$\|\boldsymbol{u}\| = \beta \tag{16f}$$

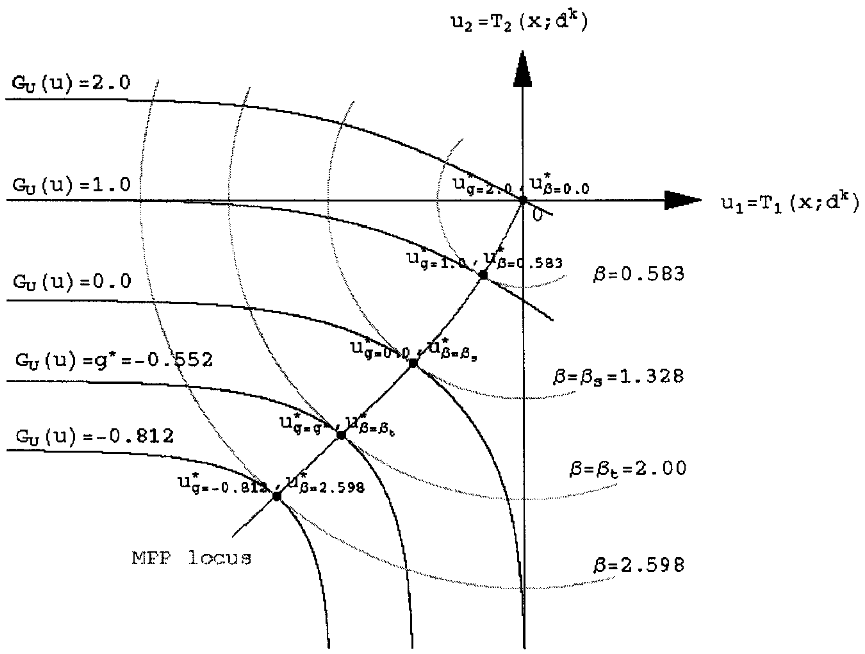

Fig. 3 MPP locus in the first-order reliability method.

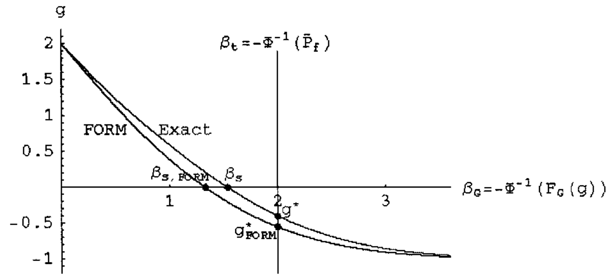

Fig. 4 Probabilistic constraint evaluation using FORM.

From another perspective, the MPP locus can also be obtained if the first-order reliability analysis is performed repeatedly for different g values as follows:
Minimize

$$\|\boldsymbol{u}\| \tag{16g}$$

subject to

$$G_U(\boldsymbol{u}) - g = 0 \tag{16h}$$

At the design $\boldsymbol{d}^k = \ 4.0, 4.0]^T$, the contours of the performance function $G_U(\boldsymbol{u}) = g$ for different g values and the MPP locus in the $\boldsymbol{u}$ space are shown in Fig. 3.

Note that the MPP $\boldsymbol{u}^*_{g=0}$ (also $\boldsymbol{u}^*_{\beta=\beta_s}$) is found in the first-order reliability analysis, whereas the MPP $\boldsymbol{u}^*_{\beta=\beta_t}$ (also $\boldsymbol{u}^*_{g=g^*}$) is found in the first-order inverse reliability analysis. These two MPPs are not coincident unless the probabilistic constraint is active. Every MPP corresponds to a point on the nonincreasing $\beta_{\text{FORM}} \sim g$ curve, which represents the FORM approximation of the exact $\beta_G \sim g$ relationship. As shown in Fig. 4, the two points $(\beta_{s,\text{FORM}}, 0)$ and $(\beta_t, g^*_{\text{FORM}})$ are exemplified by RIA and PMA, respectively.

Efficiency and Robustness of RIA and PMA

RIA and PMA search different MPPs to evaluate probabilistic constraint unless the probabilistic constraint is active. Because the MPP search in the $\boldsymbol{u}$ space usually starts from the origin, it is generally easier for numerical algorithms to find the MPP that is closer to the origin. Finding the closer MPP means searching the minimum of Eq. (15a) in a more restrictive solution space constrained by Eq. (15b). If the probabilistic constraint is violated, then $\beta_s(\boldsymbol{d}^k) < \beta_t$ and the MPP $\boldsymbol{u}^*_{g=0}$ of RIA is closer to the origin. On the other hand, if the probabilistic constraint is inactive, then $\beta_s(\boldsymbol{d}^k) > \beta_t$ and the MPP $\boldsymbol{u}^*_{\beta=\beta_t}$ of PMA is closer to the origin. The efficiencies of an MPP search in RIA and PMA become significantly different if the two MPPs are relatively far apart in the $\boldsymbol{u}$ space.

More important, RIA could yield singularity in the probabilistic constraint evaluation. At the design $\boldsymbol{d}^m = \ 4, 5]^T$, the first-order reliability analysis attempts to solve the optimization problem represented in the $\boldsymbol{x}$ space as follows:
Minimize

$$\|\boldsymbol{T}(\boldsymbol{x}; \boldsymbol{d}^k)\| \tag{17a}$$

subject to

$$G(\boldsymbol{x}) = x_1 + 2x_2 - 10 = 0 \tag{17b}$$

$$3 \le x_1 \le 5, \qquad 4 \le x_2 \le 6 \tag{17c}$$

which has no solution because Eq. (17b) conflicts with Eq. (17c). Because of zero failure probability at this design, as shown in Fig. 2, the limit-state surface is not defined in the probability integration domain. In contrast, the first-order inverse reliability analysis in PMA is well defined in the probability integration domain, and therefore, it always yields a nonsingular solution.

Unified System Space for Reliability-Based System Parameter Design

In this section, a unified system space is proposed to illustrate the close connections of the system probability analysis and RBDO. In the RBDO model, probabilistic constraints by either Eq. (8a) of RIA or Eq. (8b) of PMA are defined in the design variable space ($\boldsymbol{d}$ space), but the corresponding system performance functions are defined in the system parameter space ($\boldsymbol{x}$ space). The unified system space for reliability-based parameter design is defined by mapping the $\boldsymbol{d}$ space onto the $\boldsymbol{x}$ space as

$$\boldsymbol{x} = \boldsymbol{T}^{-1}(\boldsymbol{0}; \boldsymbol{d}) \tag{18a}$$

If all system parameters are mutually independent, this one-to-one mapping can be expressed separately for each system parameter and corresponding design variable as

$$x_i = T_i^{-1}\left(0; d_i^k\right) = F_{X_i}^{-1} \ \Phi(0)], \qquad i = 1, 2, \ldots, n \tag{18b}$$

In this unified system space, the mapping of the design $\boldsymbol{d}^k$ is $\boldsymbol{T}^{-1}$ $(\boldsymbol{0}; \boldsymbol{d}^k)$, which corresponds to the origin of the $\boldsymbol{u}$ space in the FORM definition, and three enclosed surfaces around the mapping of design $\boldsymbol{d}^k$ are defined as follows:

1) The surface of reliability target, $\|\boldsymbol{T}(\boldsymbol{x}; \boldsymbol{d}^k)\| = \beta_t$, is smooth, and its enclosed region is generally convex because it represents a monotonic transformation of the spherical surface defined by Eq. (15b) in $\boldsymbol{u}$ space.

2) The surface of reliability potential, $\|\boldsymbol{T}(\boldsymbol{x}; \boldsymbol{d}^k)\| = \beta_s(\boldsymbol{d}^k)$, is also smooth and generally convex, and $\beta_s^j(\boldsymbol{d}^k)$ is the first-order reliability index of the probabilistic constraint.

3) The surface of tolerance limits, $\|\boldsymbol{T}(\boldsymbol{x}; \boldsymbol{d}^k)\| \to \infty$, encloses the entire probability integration domain of Eq. (14e). If the performance function limit-state surface $G(\boldsymbol{x}) = 0$ is not defined inside, the failure probability of the design $\boldsymbol{d}^k$ is either zero or one.

Example 3

Consider a system described by two independent normally distributed system parameters $\boldsymbol{X} = \ X_1, X_2]^T$ with constant standard deviations $\sigma_1 = \frac{1}{2}$ and $\sigma_2 = \frac{2}{5}$. The design variable is $\boldsymbol{d} = \ d_1, d_2]^T \equiv \ \mu_1, \mu_2]^T$, and the transformation between the $\boldsymbol{u}$ space and the $\boldsymbol{x}$ space at design $\boldsymbol{d}^k$ is linear in this case as

$$u_i = T_i\left(x_i; d_i^k\right) = \Phi^{-1}\left[F_{X_i}(x_i)\right] = (x_i - d_i)/\sigma_i, \qquad i = 1, 2 \tag{19a}$$

$$x_i = T_i^{-1}\left[u_i; d_i^k\right] = F_{X_i}^{-1} \ \Phi(u_i)] = d_i^k + \sigma_i u_i, \qquad i = 1, 2 \tag{19b}$$

With the same reliability target $\beta_t^1 = \beta_t^2 = \beta_t = 2$, two probabilistic constraints are

$$P \ G_j(\boldsymbol{x}) < 0] \le \Phi\left(-\beta_t^j\right), \qquad j = 1, 2 \tag{19c}$$

where the two performance functions are defined in the $\boldsymbol{x}$ space as

$$G_1(\boldsymbol{x}) = x_1^2 x_2 \big/ 20 - 1 \tag{19d}$$

$$G_2(\boldsymbol{x}) = \left(10x_2^3 - x_1^2 x_2 - 2x_1\right) \big/ 10 - 1 \tag{19e}$$

In this example, the mapping of $\boldsymbol{d}$ space to $\boldsymbol{x}$ space can be simplified as

$$\boldsymbol{x} = \boldsymbol{T}^{-1}(\boldsymbol{0}; \boldsymbol{d}) = \boldsymbol{d} \tag{19f}$$

At design $\boldsymbol{d}^k = \ 3, 4]^T$, the probabilistic constraint evaluation in RIA is illustrated in the unified system space as shown in Fig. 5, where the first-order reliability indices of two probabilistic constraints are $\beta_s^j(\boldsymbol{d}^k) = \|\boldsymbol{T}(\boldsymbol{x}^{*,j}_{g=0}; \boldsymbol{d}^k)\|$. Conceptually, the probabilistic constraint is evaluated in RIA by fitting the surface of the reliability potential so that it is tangentially contacted with the performance function limit-state surface.

From another perspective, the probabilistic constraint evaluation in PMA is shown in Fig. 6, where the target probabilistic performance measures of two probabilistic constraints are $g_j^*(\boldsymbol{d}^k) = G(\boldsymbol{x}^{*,j}_{\beta=\beta_t})$, $j = 1, 2$. Conceptually, the probabilistic constraint is evaluated in PMA by finding the minimum performance function value on the surface of the reliability target.

Comparing Figs. 5 and 6, PMA searches MPP on the surface of the reliability target, whereas RIA searches MPP on the limit-state

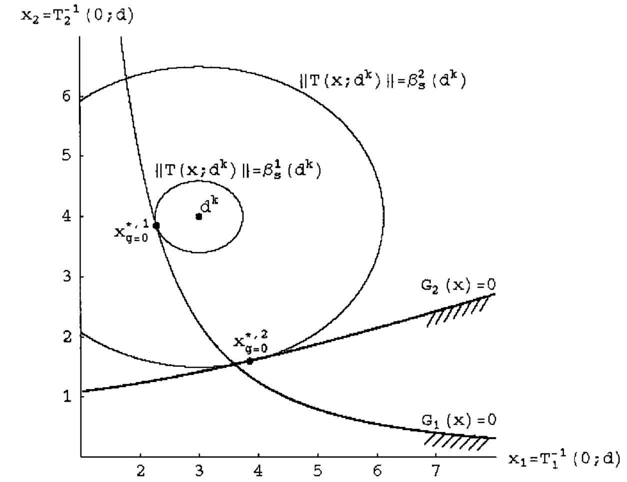

Fig. 5 Probabilistic constraint evaluations by RIA.

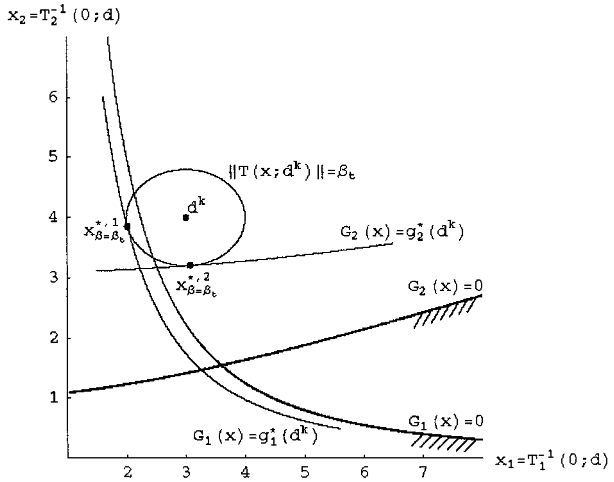

Fig. 6 Probabilistic constraint evaluations by PMA.

surface of the performance function. Thus, the search space in PMA is smaller than that in RIA if the probabilistic constraint is inactive, such as in the case of the second probabilistic constraint. On the other hand, the search space for RIA is smaller if the probabilistic constraint is violated, such as in the case of the first probabilistic constraint. Therefore, RIA is generally more efficient in dealing with violated probabilistic constraints, and PMA is more efficient for inactive constraints.

Note that the surface of the reliability target, $\|\boldsymbol{T}(\boldsymbol{x};\boldsymbol{d}^k)\|=\beta_t$, is determined only by the probability distributions of the system parameters at the design $\boldsymbol{d}^k$ and the system reliability target β_t. As shown in Fig. 7, the limit-state surface of the probabilistic constraint, $\beta_s(\boldsymbol{d})=\beta_t$ or $g^*(\boldsymbol{d})=0$), can be conceptually constructed by tangentially sweeping the surface of the reliability target along the feasible side of the performance function limit-state surface $G(\boldsymbol{x})=0$. Thus, the optimum of RBDO is the minimum cost design that can fit the surface of the reliability target into the feasible side of the active performance functions limit-state surfaces.

If the reliability target for all system performance functions is $\beta_t^j=0,\ j=1,2,\ldots,np$, then the surface of the reliability target shrinks to a point, and the RBDO problem becomes the deterministic optimization problem as follows:
Minimize

$$\text{cost}(\boldsymbol{d}) \tag{20a}$$

subject to

$$G_j(\boldsymbol{T}^{-1}(\boldsymbol{0};\boldsymbol{d}))\geq 0, \qquad j=1,2,\ldots,np \tag{20b}$$

$$\boldsymbol{d}^L\leq\boldsymbol{d}\leq\boldsymbol{d}^U \tag{20c}$$

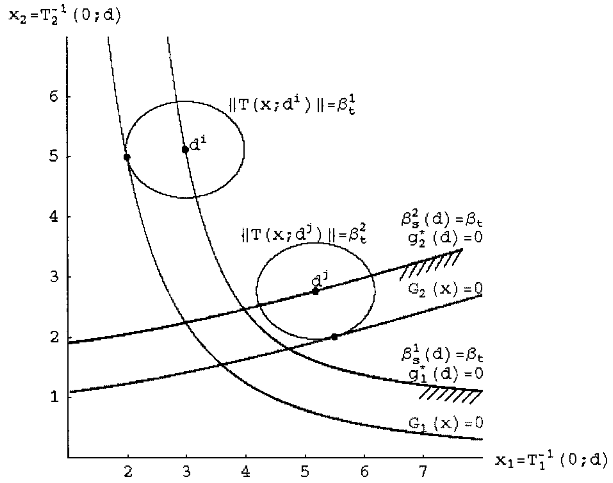

Fig. 7 Probabilistic constraint in the unified system space.

Thus, the RBDO solution space prescribed by the probabilistic constraint limited surfaces is contained inside the performance function limit-state surfaces. As the target reliability increases, the surface of reliability target expands, and consequently, the RBDO solution space becomes smaller. In practice, the optimum of the deterministic optimization problem often provides an efficient initial design for RBDO.

Example 4

If the random parameters in example 3 are uniformly distributed with the same standard deviations $\sigma_1=\frac{1}{2}$ and $\sigma_2=\frac{2}{5}$, then their CDFs can then be expressed as

$$F_{X_i}(x_i)=(x_i-d_i/2\sqrt{3}\sigma_i)+\tfrac{1}{2}$$
$$d_i-\sqrt{3}\sigma_i\leq x_i\leq d_i+\sqrt{3}\sigma_i, \qquad i=1,2 \tag{21a}$$

Thus, transformations between the $\boldsymbol{u}$ space and the $\boldsymbol{x}$ space are nonlinear as

$$u_i=T_i\big(x_i;d_i^k\big)=\Phi^{-1}\big[F_{X_i}(x_i)\big]=\Phi^{-1}\big(x_i-d_i/2\sqrt{3}\sigma_i+\tfrac{1}{2}\big) \qquad i=1,2 \tag{21b}$$

$$x_i=T_i^{-1}\big(u_i;d_i^k\big)=F_{X_i}^{-1}[\Phi(u_i)]=d_i-\sqrt{3}\sigma_i+2\sqrt{3}\sigma_i\Phi(u_i) \qquad i=1,2 \tag{21c}$$

At design $\boldsymbol{d}^k=[3,4]^T$, the evaluation of probabilistic constraints by RIA and PMA are shown in Figs. 8 and 9, respectively.

In engineering practice, the distributions of system parameters are often bounded by their tolerance limits, and therefore, the probability integration domain is finite. Note that RIA yields singularity if the limit-state surface of the performance function is defined outside of the finite probability integration domain enclosed by the surface of tolerance limits, $\|\boldsymbol{T}(\boldsymbol{x};\boldsymbol{d}^k)\|\to\infty$, as shown in Fig. 8 for the second probabilistic constraint $G_2(x)$. In contrast, PMA always has a solution because inverse reliability analysis is defined inside the probability integration domain as shown in Fig. 9. Thus, PMA is inherently more robust than RIA in probabilistic constraint evaluations.

Constrained Nonlinear Optimization Method for RBDO

Search methods (or primal methods), such as SLP, SQP, MFD, and the gradient projection method, are commonly used to solve the constrained nonlinear RBDO problem.[3–9] The search method starts with an initial design and iteratively improves it, where the search direction is evaluated by solving an approximate optimization subproblem with linearized constraints.[10,11] Because the design sensitivity information of the probabilistic constraint is a byproduct of the constraint evaluation,[15,24] SLP becomes attractive[13] for RBDO because it is usually more efficient in terms of total number of constraint evaluations. More robust search methods, such as SQP and MFD, can be used if SLP fails to converge.

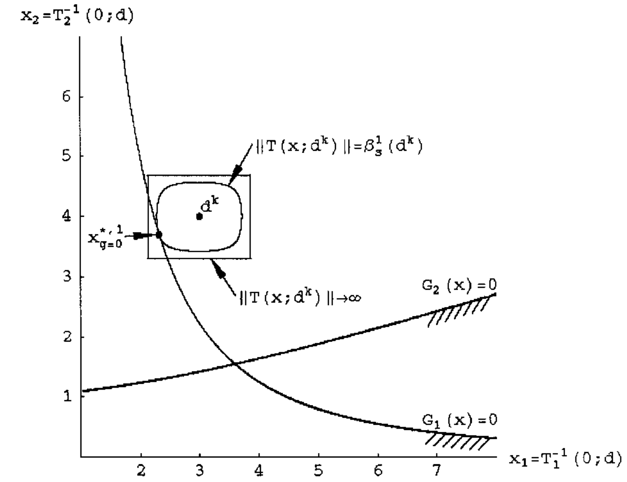

Fig. 8 RIA in the unified system space.

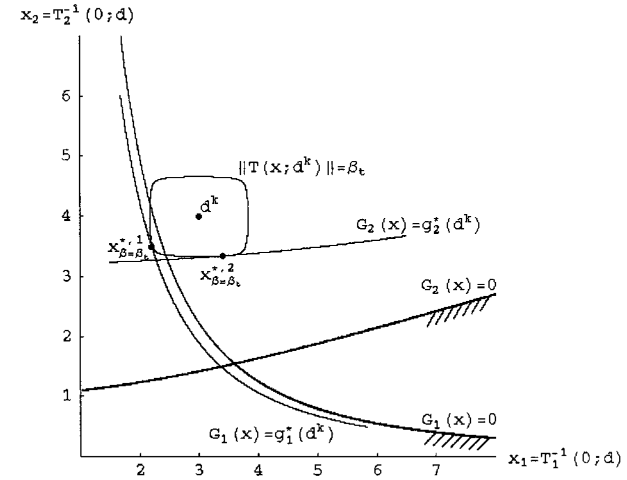

Fig. 9 PMA in the unified system space.

Design Sensitivity Analysis of Probabilistic Constraint

The probabilistic constraint evaluation in RIA or PMA is computationally intensive, but the design sensitivity of the probabilistic constraint at design $\boldsymbol{d}^k$ is readily available as a byproduct of the first-order reliability analysis in RIA and the first-order inverse reliability analysis in PMA, respectively, as

$$\nabla_d^T \beta_s(\boldsymbol{d}^k) = \frac{\nabla_d^T G_U\left(\boldsymbol{u}_{g=0}^*\right)}{\left\|\nabla_u G_U\left(\boldsymbol{u}_{g=0}^*\right)\right\|} = \frac{\nabla_d^T G\left(\boldsymbol{x}_{g=0}^*\right)}{\left\|\nabla_u G_U\left(\boldsymbol{u}_{g=0}^*\right)\right\|} \tag{22a}$$

$$\nabla_d^T g^*(\boldsymbol{d}^k) = \nabla_d^T G_U\left(\boldsymbol{u}_{\beta=\beta_t}^*\right) = \nabla_d^T G\left(\boldsymbol{x}_{\beta=\beta_t}^*\right) \tag{22b}$$

where

$$\nabla_d^T G(\boldsymbol{x}) = \left[\frac{\partial G(\boldsymbol{x})}{\partial x_i}\frac{\partial T_i^{-1}(\boldsymbol{u};\boldsymbol{d}^k)}{\partial d_i}\right]^T \tag{22c}$$

$$\nabla_u G_U(\boldsymbol{u}) = \left[\frac{\partial G(\boldsymbol{x})}{\partial x_i}\frac{\partial T_i^{-1}(\boldsymbol{u};\boldsymbol{d}^k)}{\partial u_i}\right] \tag{22d}$$

Probabilistic Constraint Approximation in the Conventional RBDO Methodology

In the conventional RBDO methodology, the probabilistic constraints are prescribed by Eq. (8a) of RIA, and the search direction determination subproblem is defined by the linearized probabilistic constraints at the current design $\boldsymbol{d}^k$. Because the design sensitivity of the probabilistic constraint is readily available as a byproduct of the probabilistic constraint evaluation, all probabilistic constraints can be included in defining the subproblem, and the linearization of

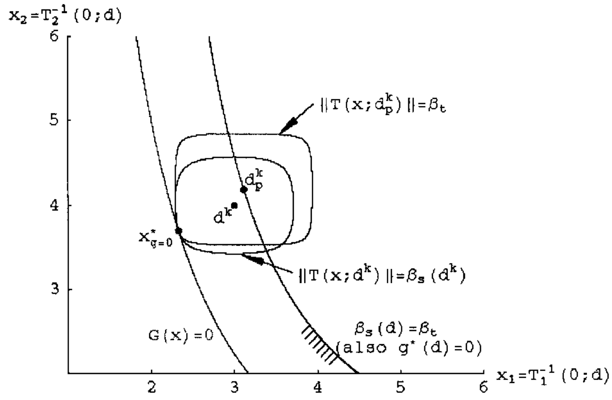

Fig. 10 Design potential method for RBDO.

a probabilistic constraint at design $\boldsymbol{d}^k$ can be expressed by Eq. (22a) as

$$\beta_s(\boldsymbol{d}^k) + \nabla_d^T \beta_s(\boldsymbol{d}^k)\cdot(\boldsymbol{d}-\boldsymbol{d}^k) \geq \beta_t \tag{23}$$

Design Potential Method for Robust System Parameter Design

The probabilistic constraint approximation at the current design essentially disconnects the close coupling of the probability analysis and RBDO of the same engineering system. When the random system probability analysis is integrated into the design optimization process, a novel design potential method (DPM) is proposed here for RBDO.

In the design optimization process, the search direction determination subproblem is defined by both linearized potential probabilistic constraints and linearized inactive probabilistic constraints. However, unlike the direct linearization at the current design point as in the conventional RBDO methodology, a potential probabilistic constraint evaluated by RIA is linearized at its DPP $\boldsymbol{d}_P^k$ in DPM.

As shown in Fig. 10, the DPP $\boldsymbol{d}_P^k$ for the potential probabilistic constraint at current design $\boldsymbol{d}^k$ is defined as the design point that renders the constraint active as

$$\beta_s\left(\boldsymbol{d}_P^k\right) = \beta_t \qquad \left[\text{or } g^*\left(\boldsymbol{d}_P^k\right) = 0\right] \tag{24}$$

and shares the same MPP of RIA $\boldsymbol{x}_{g=0}^*$ in the $\boldsymbol{x}$ space with current design $\boldsymbol{d}^k$ as

$$\boldsymbol{x}_{g=0}^* = \boldsymbol{T}^{-1}\left(\boldsymbol{u}_{g=0}^*;\boldsymbol{d}^k\right) = \boldsymbol{T}^{-1}\left(\boldsymbol{u}^{**};\boldsymbol{d}_P^k\right) \tag{25}$$

where $\boldsymbol{u}_{g=0}^*$ and $\boldsymbol{u}^{**}$ are MPPs of current design point $\boldsymbol{d}^k$ and DPP $\boldsymbol{d}_P^k$ in the $\boldsymbol{u}$ space, respectively. Because the DPP $\boldsymbol{d}_P^k$ renders the constraint active, $\boldsymbol{u}^{**}$ can be directly expressed as[15]

$$\boldsymbol{u}^{**} = -\frac{\nabla_u G_U(\boldsymbol{u}^{**})}{\left\|\nabla_u G_U(\boldsymbol{u}^{**})\right\|}\beta_t \tag{26}$$

where

$$\nabla_u G_U(\boldsymbol{u}^{**}) = \left[\frac{\partial G\left(x_{g=0}^*\right)}{\partial x_i}\frac{\partial T_i^{-1}\left(\boldsymbol{u}^{**};\boldsymbol{d}_P^k\right)}{\partial u_i}\right]$$

Thus, the potential probabilistic constraint is linearized in DPM at its DDP $\boldsymbol{d}_P^k$ as

$$\nabla_d^T \beta_s\left(\boldsymbol{d}_P^k\right)\cdot\left(\boldsymbol{d}-\boldsymbol{d}_P^k\right) \geq 0 \tag{27a}$$

where

$$\nabla_d^T \beta_s\left(\boldsymbol{d}_P^k\right) = \frac{\nabla_d^T G_U(\boldsymbol{u}^{**})}{\left\|\nabla_u G_U(\boldsymbol{u}^{**})\right\|} = \frac{\nabla_d^T G\left(\boldsymbol{x}_{g=0}^*\right)}{\left\|\nabla_u G_U(\boldsymbol{u}^{**})\right\|} \tag{27b}$$

For the inactive probabilistic constraint evaluated by PMA, the linearization using Eq. (22b) is still obtained at the current design $\boldsymbol{d}^k$ as

$$g^*(\boldsymbol{d}^k) + \nabla_d^T g^*(\boldsymbol{d}^k)\cdot(\boldsymbol{d}-\boldsymbol{d}^k) \geq 0 \tag{28}$$

Because $\boldsymbol{x}^*_{g=0}$ and $[\partial G(\boldsymbol{x}^*_{g=0})/\partial x_i]$ are already known in the MPP search for constraint evaluation, $\boldsymbol{d}^k_P$ and $\boldsymbol{u}^{**}$ can be determined by solving the nonlinear equation system comprising Eq. (25) and Eq. (26) using Newton's method (see Ref. 25). Note that solving this nonlinear equation system does not require any expensive evaluation of the system performance function $G(\boldsymbol{x})$. Terms that need to be evaluated are $\boldsymbol{T}^{-1}(\boldsymbol{u}^{**}; \boldsymbol{d}^k_P)$ and $[\partial \boldsymbol{T}_i^{-1}(\boldsymbol{u}^{**}; \boldsymbol{d}^k_P)/\partial u_i]$, which can be easily computed numerically.

Because the DDP $\boldsymbol{d}^k_P$ is located on the limit-state surface of the probabilistic constraint, the constraint approximation in DPM becomes exact at $\boldsymbol{d}^k_P$. Therefore, DPM provides better constraint approximation without additional costly evaluation of the system performance function. Consequently, a higher rate of convergence in solving the RBDO problem can be achieved.

Recall that PMA is inherently robust and is more efficient in evaluating inactive constraints, whereas RIA is more efficient for violated ones but could yield singularity for inactive ones. Therefore, an adaptive probabilistic constraint evaluation strategy has been developed by authors[13] to select adaptively either RIA or PMA in the RBDO iterations depending on the estimated marginal status of the probabilistic constraint. Note that the exact status of a probabilistic constraint is unknown until the MPP of RIA or PMA is finally found. In the adaptive strategy, PMA ensures the robustness of the evaluations of inactive probabilistic constraints, whereas RIA is used for violated and marginally active constraints so that the results can be used by DPM to accelerate the convergence of the overall RBDO process.

In the following, the first RBDO example is used to demonstrate the advantages of the DPM. Another more comprehensive RBDO example is presented to illustrate DPM for reliability-based system parameter design using adaptive probabilistic constraint evaluation. Significant improvements in terms of efficiency and robustness are shown in comparison with the conventional RBDO methodology.

Example 5

Consider a system described by two independent system parameters $\boldsymbol{X} = [X_1, X_2]^T$, where X_1 is normally distributed and X_2 is uniformly distributed. Their mean values are chosen as the design variable $\boldsymbol{d} = [d_1, d_2]^T \equiv [\mu_1, \mu_2]^T$ and their standard deviations are as $\sigma_1 = \sigma_2 = 1$. Thus, by the use of Eqs. (19a) and (19b) and Eqs. (21b) and (21c), the transformations of the $\boldsymbol{u}$ space and the x space are expressed, respectively, as

$$u_1 = x_1 - d_1$$

$$u_2 = \Phi^{-1}\big((x_2 - d_2)/2\sqrt{3} + 1/2\big) \tag{29a}$$

$$x_1 = d_1 + u_1$$

$$x_2 = d_2 - \sqrt{3} + 2\sqrt{3}\Phi(u_2) \tag{29b}$$

The RBDO problem is defined as follows:
Minimize

$$\text{cost}(\boldsymbol{d}) = -d_1 + 10d_2 \tag{29c}$$

subject to

$$P[G_j(\boldsymbol{x}) < 0] \le \Phi\big(-\beta_t^j\big), \qquad j = 1, 2 \tag{29d}$$

$$1 \le d_1 \le 10, \qquad 1 \le d_2 \le 10 \tag{29f}$$

where $\beta_t^1 = 3$ and $\beta_t^2 = 2$ and two nonlinear performance functions are defined as

$$G_1(\boldsymbol{x}) = \frac{1 - 10}{(x_1 + 2x_2)} \tag{29g}$$

$$G_2(\boldsymbol{x}) = 8 - (x_1 - 2x_2)^3 \tag{29h}$$

and the mapping of the $\boldsymbol{d}$ space to the $\boldsymbol{x}$ space can be simplified as

$$\boldsymbol{x} = \boldsymbol{T}^{-1}(\boldsymbol{0}; \boldsymbol{d}) = \boldsymbol{d} \tag{29i}$$

When starting from an arbitrarily chosen initial design $\boldsymbol{d}^0 = [6, 3]^T$, SLP can be used to solve this RBDO problem. SLP converges in one iteration if DPM is used, and the results are shown in Table 1. In contrast, it requires five iterations for SLP to converge if the conventional RBDO methodology is used, and the RBDO history is shown in Table 2.

Note that limit-state surfaces of two nonlinear performance functions are flat in $\boldsymbol{x}$ space. Moreover, the surface of the reliability target yields a constant shape for all designs in this example due to simple mapping in Eq. (29i) and the constant standard deviations. Thus, the limit-state surfaces of the probabilistic constraints are also flat in the unified system space because they can be constructed by tangentially sweeping the surface of the reliability target along the performance function limit-state surfaces.

In DPM, the probabilistic constraint is linearized about its DPP that locates on its limit-state surfaces. Hence, probabilistic constraint approximations of DPM are exact in this example, and RBDO converges in step. Note that the DPPs of the active probabilistic constraints converge to the RBDO optimum. The conventional RBDO methodology, however, approximates probabilistic constraints at the current design. Both probabilistic constraints are nonlinear even though their limit-state surfaces are flat in the unified system space. Therefore, it takes several iterations for SLP to converge.

Example 6

Consider the same system described in example 4 with the design variable $\boldsymbol{d} = [d_1, d_2]^T \equiv [\mu_1, \mu_2]^T$. The RBDO problem with reliability target $\beta_t = 2$ is defined as follows:
Minimize

$$\text{cost}(\boldsymbol{d}) = d_1 + d_2 \tag{30a}$$

subject to

$$P(G_j(\boldsymbol{x}) < 0) \le \Phi(-\beta_t), \qquad j = 1, 2, 3 \tag{30b}$$

$$1 \le d_1 \le 10, \qquad 1 \le d_2 \le 10 \tag{30c}$$

where three nonlinear performance functions are

$$G_1(\boldsymbol{x}) = x_1^2 x_2 \big/ 20 - 1 \tag{30d}$$

$$G_2(\boldsymbol{x}) = \big(10x_2^3 - x_1^2 x_2 - 2x_1\big)\big/10 - 1 \tag{30e}$$

$$G_3(\boldsymbol{x}) = 80\big/\big(x_1^2 + 8x_2 + 5\big) - 1 \tag{30f}$$

Table 2 Conventional RBDO methodology

kth Iteration	Cost	d_1^k	d_2^k	$\beta_s^1(\boldsymbol{d}^k)$	$\beta_s^1(\boldsymbol{d}^k)$
0	24.000	6.000	3.000	0.725	0.725
1	44.394	7.217	5.161	4.676	2.575
2	37.929	6.516	4.444	2.817	2.027
3	38.328	6.663	4.499	3.027	2.000
4	38.253	6.644	4.490	2.997	2.000
5	38.257	6.647	4.490	3.000	2.000
Optimum	38.257	6.647	4.490	Active	Active

Table 1 Design potential method for RBDO

kth		$\boldsymbol{d}^k$		$j = 1$			$j = 2$		
Iteration	Cost	d_1^k	d_2^k	$\beta_s^1(\boldsymbol{d}^k)$	$\boldsymbol{d}_P^k$		$\beta_s^2(\boldsymbol{d}^k)$	$\boldsymbol{d}_P^k$	
0	24.000	6.000	3.000	0.725	8.186	3.721	0.725	4.887	3.610
1	38.257	6.647	4.490	3.000	6.647	4.490	2.000	6.647	4.490
Optimum	38.257	6.647	4.490	Active	6.647	4.490	Active	6.647	4.490

Table 3 RBDO history ($d^0 =$ 5, 5]^T)

kth		d^k		RIA			PMA		
Iteration	Cost	d_1^k	d_2^k	$\beta_s^1(d^k)$	$\beta_s^2(d^k)$	$\beta_s^3(d^k)$	$g_1^*(d^k)$	$g_2^*(d^k)$	$g_3^*(d^k)$
0	10.00	5.000	5.000	——	——	1.379	2.993	67.25	——
1	8.276	4.565	3.711	——	——	——	1.286	18.86	0.186
2	7.431	4.380	2.951	——	——	——	0.572	4.705	0.346
3	6.863	4.276	2.587	——	——	——	0.257	0.828	0.442
4	6.625	4.157	2.468	2.852	2.050	——	——	——	0.500
5	6.435	4.011	2.424	1.940	2.000	——	——	——	0.551
6	6.455	4.027	2.428	2.000	2.000	——	——	——	0.546
Optimum	6.455	4.027	2.428	Active	Active	——	——	——	Inactive

Table 4 RBDO history with DPM ($d^0 =$ 3.593, 1.549]^T)

kth		d^k		$j=1$			$j=2$			$j=3$,
Iteration	Cost	d_1^k	d_2^k	$\beta_s^1(d^k)$	d_P^k		$\beta_s^2(d^k)$	d_P^k		$g_3^*(d^k)$
0	5.142	3.593	1.549	0.000	4.327	2.129	0.000	2.970	2.178	0.962
1	6.412	4.004	2.408	1.877	4.025	2.430	1.918	3.981	2.417	0.557
2	6.455	4.027	2.428	2.000	4.027	2.428	2.000	4.027	2.428	0.546
Optimum	6.455	4.027	2.428	Active	4.027	2.428	Active	4.027	2.428	Inactive

Table 5 RBDO history without DPM ($d^0 =$ 3.593, 1.549]^T)

kth		d^k		RIA			PMA		
Iteration	Cost	d_1^k	d_2^k	$\beta_s^1(d^k)$	$\beta_s^2(d^k)$	$\beta_s^3(d^k)$	$g_1^*(d^k)$	$g_2^*(d^k)$	$g_3^*(d^k)$
0	5.142	3.593	1.549	0.000	0.000	——	——	——	0.962
1	6.829	4.034	2.795	——	——	——	0.202	3.526	0.461
2	6.648	4.132	2.516	3.035	2.477	——	——	——	0.496
3	6.410	3.979	2.431	1.864	2.099	——	——	——	0.559
4	6.461	4.032	2.429	2.025	2.002	——	——	——	0.544
5	6.452	4.025	2.428	1.995	2.000	——	——	——	0.546
6	6.455	4.027	2.428	2.000	2.000	——	——	——	0.546
Optimum	6.455	4.027	2.428	Active	Active	——	——	——	Inactive

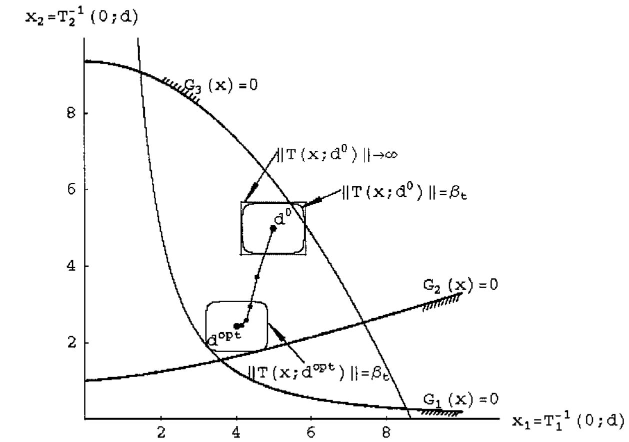

Fig. 11 RBDO history in unified system space.

Case 1: RBDO Starting at Arbitrary Initial Design $d^0 =$ 5, 5]^T

As illustrated in the unified system space shown in Fig. 11, RIA yields singularity in evaluating some probabilistic constraints at the initial design because their limit-state surfaces are not defined in the finite probability integration domain bounded by the surface of tolerance limits, $\|T(x; d^k)\| \to \infty$. Thus, the conventional RBDO methodology cannot be used directly to solve this RBDO problem.

Using the adaptive probabilistic constraint evaluation, SLP can be used to solve the problem. The RBDO history is shown in Fig. 11 and listed in Table 3, where RIA and PMA are used adaptively depending on the status of the probabilistic constraints. In the last three iterations, the adaptive MPP search algorithm chooses RIA to evaluate the first and second probabilistic constraints and DPM is used to accelerate the convergence of RBDO. The optimum of this RBDO problem is $d^{\text{opt}} =$ 4.027, 2.428]^T.

Case 2: RBDO Starting at Selective Initial Design $d^0 =$ 3.593, 1.549]^T

The optimum of the deterministic optimization problem usually provides an effective initial design for RBDO. The initial design $d^0 =$ 3.593, 1.549]^T is obtained as follows:
Minimize

$$\text{cost}(d) \tag{31a}$$

subject to

$$G_j(d) \geq 0, \qquad j = 1, 2, 3 \tag{31b}$$

$$1 \leq d_1 \leq 10, \qquad 1 \leq d_2 \leq 10 \tag{31c}$$

which can be solved by a constrained optimization method, such as SLP, SQP, and MFD.

Using DPM with adaptive probabilistic constraint evaluation, this case can be solved by SLP, and the RBDO history is shown in Table 4. Because potential probabilistic constraints at the initial design are also active probabilistic constraints at the RBDO optimum, RBDO can take full advantage of DPM and, therefore, converge much quickly than starting from $d^0 =$ 5, 5]^T.

For comparison, it is also solved using adaptive probabilistic constraint evaluation without DPM, which takes significantly more iterations to converge, as shown in Table 5. Note that RIA yields singularity in evaluating all three probabilistic constraints at 4.034, 2.795]^T in iteration 1, as shown in Table 5.

Case 3: RBDO with High Reliability Target ($\beta_t = 3$)

The advantage of DPM becomes more significant in dealing with a design problem with high reliability requirements. By changing the reliability target from $\beta_t = 2$ to $\beta_t = 3$, the RBDO history with DPM is listed in Table 6. Note that the DPPs of the active probabilistic constraints converge to the RBDO optimum. Without DPM, the RBDO takes many more iterations to converge, as shown in Table 7. The

Table 6 RBDO history with DPM ($\beta_t = 3$)

kth Iteration	Cost	$\boldsymbol{d}^k$		$j=1$			$j=2$			$j=3$,
		d_1^k	d_2^k	$\beta_s^1(\boldsymbol{d}^k)$	$\boldsymbol{d}_P^k$		$\beta_s^2(\boldsymbol{d}^k)$	$\boldsymbol{d}_P^k$		$g_3^*(\boldsymbol{d}^k)$
0	5.142	3.593	1.549	0.000	4.431	2.218	0.000	2.782	2.229	0.888
1	6.600	4.082	2.518	2.618	4.105	2.542	2.648	4.041	2.530	0.462
2	6.647	4.102	2.545	2.985	4.102	2.546	3.000	4.102	2.545	0.452
3	6.648	4.103	2.545	3.000	4.103	2.545	3.000	4.103	2.545	0.452
Optimum	6.648	4.103	2.545	Active	4.103	2.545	Active	4.103	2.545	Inactive

Table 7 RBDO history without DPM ($\beta_t = 3$)

kth Iteration	Cost	$\boldsymbol{d}^k$		RIA			PMA		
		d_1^k	d_2^k	$\beta_s^1(\boldsymbol{d}^k)$	$\beta_s^2(\boldsymbol{d}^k)$	$\beta_s^3(\boldsymbol{d}^k)$	$g_1^*(\boldsymbol{d}^k)$	$g_2^*(\boldsymbol{d}^k)$	$g_3^*(\boldsymbol{d}^k)$
0	5.142	3.593	1.549	0.000	0.000	——	——	——	0.888
1	7.671	4.254	3.417	——	——	——	0.603	11.47	0.257
2	7.193	4.339	2.854	——	——	——	0.339	2.475	0.334
3	6.931	4.300	2.631	——	——	——	0.176	0.300	0.384
4	6.773	4.201	2.572	——	3.033	——	0.077	——	0.420
5	6.700	4.145	2.555	——	2.986	——	0.032	——	0.438
6	6.670	4.122	2.548	3.321	2.951	——	——	——	0.445
7	6.629	4.088	2.541	2.811	2.995	——	——	——	0.456
8	6.651	4.105	2.546	3.040	3.003	——	——	——	0.451
9	6.647	4.102	2.545	2.985	3.000	——	——	——	0.452
10	6.648	4.103	2.545	3.000	3.000	——	——	——	0.452
Optimum	6.648	4.103	2.545	Active	Active	——	——	——	Inactive

optimum of this RBDO problem is $\boldsymbol{d}^{\text{opt}} = [4.103, 2.545]^T$, which is more conservative than the optimum corresponding to $\beta_t = 2$ of the preceding case.

The advantage of the adaptive probabilistic constraint evaluation can also be noticed in Table 7. Even without considering the third constraint, RIA yields singularity in dealing with probabilistic constraints that are eventually active, as shown from iterations 1–5. The RIA can be used to solve this RBDO problem only if the initial design is very close to optimum, such as choosing $\boldsymbol{d}^0 = [4.122, 2.548]^T$. However, this is very unlikely in practical applications.

Conclusions

The robust system parameter design in RBDO includes two closely coupled components, the probability analysis in the constraint evaluation and the iterative design optimization process. The conventional RBDO methodology essentially disconnects their relationship by directly applying the well-established reliability analysis and design optimization methods.

From a design perspective, it is shown that the probabilistic constraints that are imposed on the individual failure modes can be effectively evaluated by conventional RIA and proposed PMA. The PMA is inherently robust and is more efficient if the probabilistic constraint is inactive at the current design, whereas RIA is more efficient if the constraint is violated. Moreover, by integrating system probability analysis into the design optimization process as illustrated in the proposed unified system space, DPM is developed for highly effective probabilistic constraint approximation. The DPM can significantly improve the RBDO rate of convergence because it takes advantage of the important design information unveiled in the reliability analysis for the probabilistic constraint evaluation.

Using DPM with adaptive probabilistic constraint evaluation strategy, it is concluded that the proposed RBDO methodology for reliability-based system parameter design is not only inherently robust but is also significantly more efficient than the conventional RBDO methodology and, therefore, can be used effectively in engineering practice.

Acknowledgment

This research is partially supported by the Automotive Research Center sponsored by the U.S. Army TARDEC.

References

[1] Buck, R. J., and Wynn, H. P., "Optimization Strategies in Robust Engineering Design and Computer-Aided Design," *Quality and Reliability Engineering International*, Vol. 9, No. 1, 1993, pp. 39–48.

[2] Yang, K., Xie, W., and He, Y., "Parameter and Tolerance Design in the Engineering Modeling Stage," *International Journal of Production Research*, Vol. 32, No. 12, 1994, pp. 2803–2816.

[3] Enevoldsen, I., "Reliability-Based Optimization as an Information Tool," *Mechanics of Structures and Machines*, Vol. 22, No. 1, 1994, pp. 117–135.

[4] Enevoldsen, I., and Sorensen, J. D., "Reliability-Based Optimization in Structural Engineering," *Structural Safety*, Vol. 15, No. 3, 1994, pp. 169–196.

[5] Chandu, S. V. L., and Grandi, R. V., "General Purpose Procedure for Reliability Based Structural Optimization Under Parametric Uncertainties," *Advances in Engineering Software*, Vol. 23, No. 1, 1995, pp. 7–14.

[6] Frangopol, D. M., and Corotis, R. B., "Reliability-Based Structural System Optimization: State-of-the-Art versus State-of-the-Practice," *Analysis and Computation: Proceedings of the Twelfth Conference held in Conjunction with Structures Congress XIV*, edited by F. Y. Cheng, American Society of Civil Engineers, Chicago, 1996, pp. 67–78.

[7] Wu, Y.-T., and Wang, W., "A New Method for Efficient Reliability-Based Design Optimization," *Probabilistic Mechanics and Structural Reliability: Proceedings of the 7th Special Conference*, edited by D. M. Frangopol and M. D. Grigoriu, American Society of Civil Engineers, Worcester, MA, 1996, pp. 274–277.

[8] Grandhi, R. V., and Wang, L., "Reliability-Based Structural Optimization Using Improved Two-Point Adaptive Nonlinear Approximations," *Finite Elements in Analysis and Design*, Vol. 29, 1998, pp. 35–48.

[9] Yu, X., Choi, K. K., and Chang, K. H., "A Mixed Design Approach for Probabilistic Structural Durability," *Journal of Structural Optimization*, Vol. 14, No. 2–3, 1997, pp. 81–90.

[10] Arora, J. S., *Introduction to Optimum Design*, McGraw–Hill, New York, 1989, Chaps. 5–6.

[11] Haftka, R. T., and Gurdal, Z., *Elements of Structural Optimization*, Klumer Academic, Dordrecht, The Netherlands, 1991, Chaps. 2–3.

[12] Tu, J., Choi, K. K., and Park, Y. H., "A New Study on Reliability-Based Design Optimization," *Journal of Mechanical Design*, Vol. 121, No. 4, 1999, pp. 557–564.

[13] Tu, J., and Choi, K. K., "Design Potential Concept for Reliability-Based Design Optimization," Center for Computer-Aided Design, TR. R99-07, Univ. of Iowa, Iowa City, IA, Dec. 1999.

[14] Scheaffer, R. L., and McClave, J. T., *Probability and Statistics for Engineers*, PWS-KENT, Boston, MA, 1990, Chaps. 2–3.

[15] Madsen, H. O., Krenk, S., and Lind, N. C., *Methods of Structural Safety*, Prentice–Hall, Englewood Cliffs, NJ, 1986, Chaps. 4–5.

[16] Rubinstein, R. Y., *Simulation and the Monte Carlo Method*, Wiley, New York, 1981, Chaps. 3–5.

[17] Rosenblatt, M., "Remarks on a Multivariate Transformation," *Annals of Mathematical Statistics*, Vol. 23, 1952, pp. 470–472.

[18]Hohenbichler, M., and Rackwitz, R., "Nonnormal Dependent Vectors in Structural Reliability," *Journal of the Engineering Mechanics Division, ASCE*, Vol. 107, No. 6, 1981, pp. 1127–1238.

[19]Liu, P. L., and Kiureghian, A. D., "Optimization Algorithms for Structural Reliability," *Structural Safety*, Vol. 9, No. 3, 1991, pp. 161–177.

[20]Wu, Y.-T., and Wirsching, P. H., "New Algorithm for Structural Reliability Estimation," *Journal of Engineering Mechanics*, Vol. 113, No. 3, 1987, pp. 1319–1336.

[21]Wu, Y.-T., Millwater, H. R., and Cruse, T. A., "An Advanced Probabilistic Structural Analysis Method for Implicit Performance Functions," *AIAA Journal*, Vol. 28, No. 9, 1990, pp. 1663–1669.

[22]Wang, L. P., and Grandhi, R. V., "Efficient Safety Index Calculation for Structural Reliability Analysis," *Computer and Structures*, Vol. 52, No. 1, 1994, pp. 103–111.

[23]Wu, Y.-T., "Computational Methods for Efficient Structural Reliability and Reliability Sensitivity Analysis," *AIAA Journal*, Vol. 32, No. 8, 1994, pp. 1717–1723.

[24]Yu, X., Chang, K. H., and Choi, K. K., "Probabilistic Structural Durability Prediction," *AIAA Journal*, Vol. 36, No. 4, 1998, pp. 628–637.

[25]Atkinson, K. E., *An Introduction to Numerical Analysis*, Wiley, New York, 1989, Chap. 2.

E. R. Johnson
Associate Editor